

## Bicriticality in $\text{Fe}_x\text{Co}_{1-x}\text{Ta}_2\text{O}_6$

E. J. Kinast,<sup>1</sup> V. Antonietti,<sup>1</sup> D. Schmitt,<sup>2</sup> O. Isnard,<sup>3</sup> J. B. M. da Cunha,<sup>1</sup> M. A. Gusmão,<sup>1</sup> and C. A. dos Santos<sup>1,\*</sup>

<sup>1</sup>*Instituto de Física, Universidade Federal do Rio Grande do Sul, C.P. 15051, 91501-970 Porto Alegre, Brazil*

<sup>2</sup>*Laboratoire L. Néel, CNRS, BP 166, 38042 Grenoble Cedex 09, France*

<sup>3</sup>*Laboratoire de Cristallographie, CNRS, associé à l'Université J. Fourier et à l'INPG, B.P. 166, 38042 Grenoble Cedex 9, France*

(Received 19 March 2003; published 6 November 2003)

X-ray and neutron-diffraction, dc magnetic susceptibility, magnetization, and specific-heat measurements are reported for  $\text{Fe}_x\text{Co}_{1-x}\text{Ta}_2\text{O}_6$  mixed oxides. X-ray refinement indicates homogeneous samples for all the reported concentrations. The neutron-diffraction measurements reveal magnetic structures with double propagation vectors  $(\pm 1/4, 1/4, 1/4)$  for  $\text{CoTa}_2\text{O}_6$ , and  $(1/2, 0, 1/2)$  and  $(0, 1/2, 1/2)$  for  $\text{FeTa}_2\text{O}_6$ . The latter remain unchanged in the Fe-rich samples, for  $0.46 \leq x < 1.00$ , while the Co-rich samples show propagation vectors  $(\pm 1/4, 1/4, 0)$  for  $0.09 \leq x < 0.46$ . The temperature vs  $x$  phase diagram exhibits a bicritical point at about  $T = 4.9$  K and  $x = 0.46$ . For this concentration, and at low temperatures, the system shows coexistence of both magnetic structures. This novel bicritical behavior is interpreted as induced by competition between the different magnetic and crystallographic structures.

DOI: 10.1103/PhysRevLett.91.197208

PACS numbers: 75.30.Kz, 64.75.+g, 83.85.Hf

In general terms, the phenomenon of phase separation is related to a competition between two ordered states. Typical phase diagrams consist of three regions, corresponding to the high-temperature state and the two different ground states. As the temperature is lowered, the system undergoes a second-order transition from the homogeneous high-temperature phase to either of the competing ordered phases. Thus, a bicritical point exists in the phase diagram where the two second-order transition lines meet a first-order one separating the ordered states.

Spatial phase separation in magnetic semiconductors was theoretically predicted by Nagaev [1] in the early 1970's. Lately, interest in the subject has been revived in connection with the observation of stripe phases in high-temperature superconductors, and various types of phase coexistence in colossal-magnetoresistance manganites [2–7]. Competition in these systems mostly occurs between ferromagnetic (FM) and antiferromagnetic (AF) phases, but also between charge-ordered and charge-exchange states, or between charge/orbital ordering and FM states [2]. In this context, a bicritical point was clearly observed, for example, in  $\text{Pr}_{0.55}(\text{Ca}_{1-x}\text{Sr}_x)_{0.45}\text{MnO}_3$  [5].

Initially, the observation of phase separation was related to chemical inhomogeneities, but its evidence in single crystals of  $\text{Sr}_3\text{CuIrO}_6$  [8] suggested that its occurrence was more widespread, not restricted to a small number of materials nor to chemically inhomogeneous compounds. Dagotto *et al.* [2] pointed out that coexistence of competing phases is an intrinsic feature in manganites, unrelated to grain-boundary effects of polycrystals, and that its theoretical understanding and experimental control is a challenge that should be strongly pursued. Recently [9], spatially separated phases

were directly observed via electron microscopy in  $\text{La}_{0.5}\text{Ca}_{0.5}\text{MnO}_3$ .

In this Letter, we present results evidencing the existence of a bicritical point for a different type of insulating material,  $\text{Fe}_x\text{Co}_{1-x}\text{Ta}_2\text{O}_6$ , whose sample preparation and structure refinement have been recently reported [10,11].

Accurate x-ray measurements at room temperature show that all the samples are single phase (no spurious reflections) and homogeneous (no abnormal line broadening as a function of the diffraction angle), therefore characterizing an unlimited and homogeneous solid solution. Detailed crystallographic studies of this kind of compounds can be found in the literature [12]. The system crystallizes in the trirutile structure with space group  $P4_2/mnm$ . In this structure,  $\text{Fe}^{2+}$  or  $\text{Co}^{2+}$  and  $\text{Ta}^{5+}$  ions are surrounded by  $\text{O}^{2-}$  octahedra. This yields Fe/Co-O layers (at  $z = 0$  and  $z = 1/2$ ) separated by two Ta-O layers (at  $z \sim 1/6$  and  $z \sim 1/3$ ). According to Eicher *et al.* [12], the magnetic structure for  $\text{FeTa}_2\text{O}_6$  consists of two families of AF planes, the anisotropy axis of one family being rotated by  $90^\circ$  with respect to the other, and a 3D magnetic lattice is observed which can be viewed as a stack of alternating planes of each family. The anisotropy-axis direction on the basal plane correlates well with the symmetry of the local field originating from the oxygen atoms surrounding each Fe atom in the lattice. On the other hand, according to Reimers *et al.* [13], magnetic order in  $\text{CoTa}_2\text{O}_6$  can be better described as a complex helical spin structure with components on the basal plane as well as in the  $c$  direction. It was the perspective of obtaining a mixed oxide with competing anisotropies that motivated us to undertake the present investigation. Surprisingly, our results show that anisotropy plays a minor role in the observed bicriticality, which is due to

competing AF interactions modified by changes in the lattice parameters.

Direct-current magnetic susceptibilities ( $\chi$ ) were measured in an extraction magnetometer, for temperatures in the range from 1.5 to 50 K, at a constant magnetic field  $\mu_0 H = 0.5$  T in the field-cooled state. Specific-heat measurements were performed with an ac calorimeter at temperatures ranging from 4.2 to 25 K. The behavior of  $\chi$  above 50 K was obtained by extrapolating the magnetization versus field data down to zero applied field at several temperatures between 50 and 300 K. Neutron powder-diffraction experiments were made with the CRG-D1B diffractometer operated by the CNRS at the Institute Laue Langevin, in Grenoble, France. These measurements were performed with wavelength  $\lambda = 2.52$  Å in the angular range from  $16^\circ$  to  $96^\circ$  with steps of  $0.2^\circ$  at temperatures from 1.5 to 100 K. Crystal and magnetic structures were refined using the FULLPROF program [14].

A typical susceptibility vs temperature curve for one of the studied samples is shown in Fig. 1. Similar curves were obtained for all samples, in agreement with previous results for  $\text{FeTa}_2\text{O}_6$  [15]. The Néel temperature,  $T_N$ , is marked by an abrupt change of slope in the susceptibility curve, coinciding with the position of a sharp peak observed in the specific-heat data. As can be seen in Fig. 1, the susceptibility presents a relatively broad maximum just above  $T_N$ , which indicates the presence of enhanced short-range correlations characteristic of a low-dimensional material. This should actually be expected on the basis of the stacking-planes structure described above. Indeed, we were able to fit the susceptibility data almost down to  $T_N$  (solid line in Fig. 1) using a high-temperature series expansion for a Heisenberg antiferromagnet with competing nearest-neighbor ( $J_1$ ) and next-nearest-neighbor ( $J_2$ ) AF interactions on a 2D square lattice, including a single-ion anisotropy term

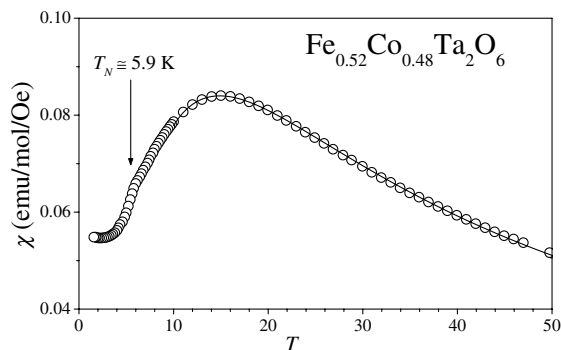


FIG. 1. Variation of the uniform magnetic susceptibility as a function of temperature for the indicated sample. The arrow indicates the slope change that occurs at the Néel temperature. Circles are experimental data, while the solid line is a fitting to a two-dimensional Heisenberg model, as briefly described in the text.

related to an in-plane easy axis [16]. It is worth mentioning that the Fe/Co-O planes were described by the same model for all concentrations, with the uniaxial anisotropy strength  $D$  varying from a highest value for pure Co to a lowest value for pure Fe, but always large enough to guarantee that the spins lay along the easy axis in each plane. Besides, the best-fitting ratio  $J_2/J_1$  never departed much from unity, in contrast to other calculations [13,17,18], and  $J_1 \approx J_2$  for  $x \approx 0.4$ .

Our main result is the  $T \times x$  phase diagram shown in Fig. 2. It can be seen that  $T_N$  values for the Fe-rich region ( $x > 0.46$ ) decrease from 9.5 to 4.9 K, while for the Co-rich region  $T_N$  varies from 7.1 to 4.9 K. It is also clear that the  $\text{Fe}_{0.46}\text{Co}_{0.54}\text{Ta}_2\text{O}_6$  sample lies at or close to a bicritical point corresponding to  $T \approx 4.9$  K. The magnetic structures below  $T_N$  were assessed by neutron-diffraction measurements down to 1.5 K and are identified by their propagation vectors, as will be discussed in detail below. Except for  $\text{Fe}_{0.46}\text{Co}_{0.54}\text{Ta}_2\text{O}_6$ , all the samples showed to be single phase with respect to both crystal and magnetic structures. There is no evidence of mixed phases at any temperature for all the other sample. In contrast,  $\text{Fe}_{0.46}\text{Co}_{0.54}\text{Ta}_2\text{O}_6$  exhibited a single crystallographic phase but coexistence of two magnetic phases. Such results are illustrated in Fig. 3 for samples  $\text{Fe}_{0.36}\text{Co}_{0.64}\text{Ta}_2\text{O}_6$ ,  $\text{Fe}_{0.46}\text{Co}_{0.54}\text{Ta}_2\text{O}_6$ , and  $\text{Fe}_{0.52}\text{Co}_{0.48}\text{Ta}_2\text{O}_6$ . For  $x = 0.46$  and  $T = 1.5$  K, we can determine that 62% of the system is in the phase characterized by the propagation vectors  $(\pm 1/4, 1/4, 0)$ , while the remaining 38% corresponds to the vectors  $(1/2, 0, 1/2)$  and  $(0, 1/2, 1/2)$ . This holds with little variation (less than 2%) up to 4 K, along the vertical line shown in Fig. 2, although the average local moment

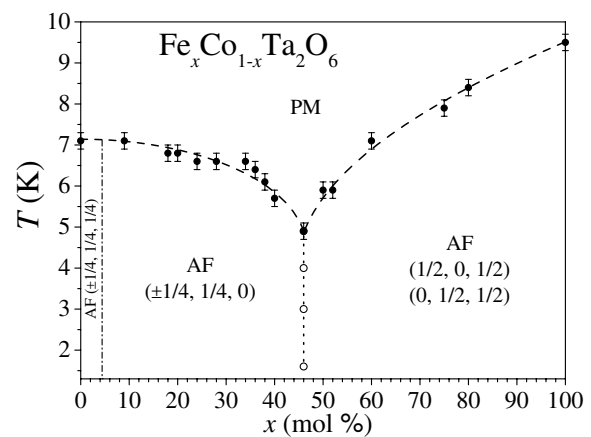


FIG. 2.  $T$  vs Fe concentration phase diagram. Solid circles are  $T_N$  obtained from magnetic susceptibility measurements and open circles were obtained from neutron diffraction on the  $\text{Fe}_{0.46}\text{Co}_{0.54}\text{Ta}_2\text{O}_6$  sample. Broken lines are guides to the eye. The two AF ordered states are labeled by their propagation vectors (see text). The dash-dotted vertical line has been arbitrarily positioned, since only the sample with  $x = 0$  lies inside that region.

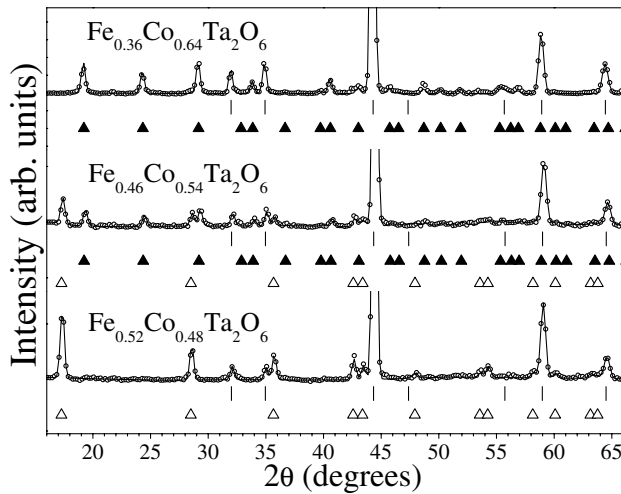


FIG. 3. Neutron diffraction pattern taken at 1.5 K for samples near the bicritical point. The bars are crystallographic Bragg reflections; solid triangles are magnetic reflections indexed by the propagation vectors  $(\pm 1/4, 1/4, 0)$ ; open triangles are magnetic reflections indexed by the propagation vectors  $(1/2, 0, 1/2)$  and  $(0, 1/2, 1/2)$ . Notice that only the middle sample shows reflections from both magnetic structures.

is reduced in both phases as the temperature rises. Notice that this vertical line fixed at  $x = 0.46$  is not a true first-order line, although we know for sure that its points are located inside the coexistence region of the two phases. From our sample set we cannot determine the precise width of this coexistence region. We can only ascertain that it is confined within the range  $0.36 < x < 0.52$ , since the two limiting samples unambiguously show a single phase, as can be seen in Fig. 3.

It is interesting to notice that our phase diagram, Fig. 2, is astonishingly similar to the one obtained by Tomioka and Tokura for  $\text{Pr}_{0.55}(\text{Ca}_{1-x}\text{Sr}_x)_{0.45}\text{MnO}_3$  [5]. However, the phases involved are completely different in nature: the phase boundary in the above manganites is between charge/orbital-ordered and FM states, while here both Co-rich and Fe-rich compounds are AF, but with different propagation vectors. Thus, we expect the phase coexistence to be related to some subtle competition between magnetic interactions.

We now turn to a more detailed discussion of the ordered phases. In order to better describe the magnetic structure we will refer to the conventional crystallographic unit cell, which is body centered tetragonal, with magnetic ions at the corners and center, i.e., positions  $000$  and  $\frac{1}{2}\frac{1}{2}\frac{1}{2}$ , respectively. Then, the samples with  $x < 0.46$  present a magnetic structure that can be described by two propagation vectors:  $(1/4, 1/4, 0)$  with  $M_0 \parallel [110]$ , referring, e.g., to the magnetic moments of corner ions, and  $(-1/4, 1/4, 0)$  with  $M_0 \parallel [\bar{1}10]$ , describing the magnetic moments of center ions. Two neighboring planes of this arrangement are depicted in Fig. 4(a). It can be observed that the two types of planes are stacked

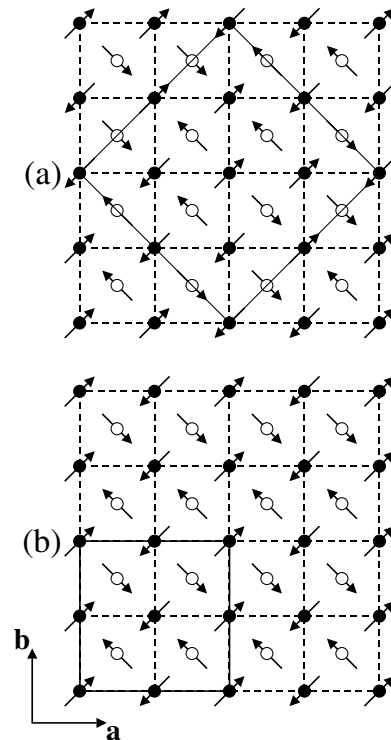


FIG. 4. Schematic representation of (a) Co- and (b) Fe-rich magnetic structures along the  $ab$  planes. Filled and open circles represent magnetic ions at positions  $000$  and  $\frac{1}{2}\frac{1}{2}\frac{1}{2}$  of the crystallographic unit cell, respectively. The Co-rich structure is described by the propagation vectors  $(\pm 1/4, 1/4, 0)$ , while the Fe-rich one is described by  $(1/2, 0, 1/2)$  and  $(0, 1/2, 1/2)$ . Dashed lines are limits of crystallographic unit cells, while the magnetic unit cells for each structure are depicted with solid lines.

in an alternating sequence, with the spins in each family being rotated by  $90^\circ$  with respect to the other. Notice that this structure is different from that obtained by Reimers *et al.* for  $\text{CoTa}_2\text{O}_6$  [13]. Actually, for  $\text{CoTa}_2\text{O}_6$  we obtain a more complex structure, with propagation vectors  $(\pm 1/4, 1/4, 1/4)$ , while the two-family structure described above appears for  $0.09 \leq x < 0.46$ . On the other hand, for  $x > 0.46$  we find the same structure obtained by Eicher *et al.* for  $\text{FeTa}_2\text{O}_6$  [12], with propagation vectors  $(1/2, 0, 1/2)$  and  $(0, 1/2, 1/2)$  for atoms located at  $000$  and  $\frac{1}{2}\frac{1}{2}\frac{1}{2}$ , respectively, as illustrated in Fig. 4(b). Thus, roughly speaking, we observe two double-vector structures, one for cobalt-rich and another for iron-rich samples. In the borderline between these two regimes,  $\text{Fe}_{0.46}\text{Co}_{0.54}\text{Ta}_2\text{O}_6$  shows coexistence of both magnetic phases.

As we mentioned before, the observed phase separation should be naturally interpreted as due to competition between magnetic interactions. This, in turn, should be related to crystallographic changes in the samples which affect the exchange constants and single-ion anisotropy. In fact, the model parameters that we use to fit our

susceptibility data vary smoothly with  $x$ . More specifically, both  $J_1$  and  $J_2$  are reduced in absolute value, but the variation of the latter is more pronounced, such that the ratio  $\alpha \equiv J_2/J_1$  decreases from  $\alpha > 1$  for Co-rich samples to  $\alpha < 1$  for Fe-rich ones. However, the strongest variation occurs in the anisotropy strength  $D$ , indicating that the oxygen octahedra surrounding each magnetic ion are being reshaped. In this sense, it is interesting to observe the behavior of the distortion index, defined as

$$\kappa = \frac{O2-O2 - O1-O1}{\langle Oi-Oi \rangle} \times 100,$$

where  $Oi-Oi$  stands for the bond length between equivalent oxygen ions in the  $AB_2O_6$  structure [11]. In the low-temperature region, where the ordered phases compete,  $\kappa$  increases with  $x$ , which means that the octahedra are shortening along the O1-A-O1 diagonal, A being the magnetic atom (either Fe or Co). Thus, the main effect on the exchange parameters is probably due to variations of the bond angle of A-O-A superexchange interactions. These considerations are not sufficient to infer what magnetic structures should be expected. Given that anisotropy axes are fixed in each plane, a simple counting of bond energies allows us to verify that the in-plane orderings shown in Fig. 4 are energetically favored over the Néel state for the corresponding sets of parameters within the model utilized here. However, for  $x \sim 0.4$  the exchange constants  $J_1$  and  $J_2$  become approximately equal, leading to frustration of the 2D order. In any case, since the overall magnetic structure is clearly three dimensional, interplane coupling must play an important role in stabilizing the ordered states. Unfortunately, a full 3D model for the magnetic interactions in such systems is not available at present. We can speculate only that variations of interplane coupling due to deformation of the oxygen octahedra could yield different ordered states depending on the concentration, since this coupling also involves superexchange through the oxygen atoms.

In conclusion, we have shown that the antiferromagnetic insulating compound  $Fe_{0.46}Co_{0.54}Ta_2O_6$ , which presents typical two-dimensional magnetic behavior above  $T_N$ , also exhibits magnetic phase separation below this temperature. This compound is near the borderline between two distinct AF magnetic regimes observed in the family of compounds  $Fe_xCo_{1-x}Ta_2O_6$ , for which a bicritical point appears in the  $T \times x$  phase diagram. We suggest that this behavior is caused by a complex competition between intra- and interplane exchange interactions in the presence of strong anisotropy.

We would like to thank Dr. Christophe Marcenat (CEA-Grenoble, DRFMC/SPSMS/LCP) for the  $C_P$  measurements. This work was supported in part by the Brazilian agencies CAPES and CNPq.

---

\*Electronic address: cas@if.ufrgs.br

- [1] E. L. Nagaev, Pis'ma Zh. Eksp. Teor. Fiz. **16**, 558 (1972) [JETP Lett. **16**, 394 (1972)]; V. A. Kashin and E. L. Nagaev, Zh. Eksp. Teor. Fiz. **66**, 2105 (1974) [Sov. Phys. JETP **39**, 1036 (1974)]; see also E. L. Nagaev, J. Magn. Magn. Mater. **140-144**, 1277 (1995); Phys. Rev. B **64**, 14 401 (2001).
- [2] E. Dagotto, T. Hotta, and A. Moreo, Phys. Rep. **344**, 1 (2001).
- [3] M. Uehara and S.-W. Cheong, Europhys. Lett. **52**, 674 (2000).
- [4] J. Lorenzana, C. Castellani, and C. di Castro, Europhys. Lett. **57**, 704 (2002).
- [5] Y. Tomioka and Y. Tokura, Phys. Rev. B **66**, 104416 (2002).
- [6] J. Hejtmánek, Z. Jiráček, M. Maryško, C. Martin, A. Maignan, and Y. Tomioka, J. Appl. Phys. **91**, 7727 (2002).
- [7] R. S. Freitas, L. Ghivelder, P. Levy, and F. Parisi, Phys. Rev. B **65**, 104403 (2002).
- [8] A. Niazi, P. L. Paulose, and E. V. Sampathkumaran, Phys. Rev. Lett. **88**, 107202 (2002).
- [9] J. C. Loudon, N. D. Mathur, and P. A. Midgley, Nature (London) **420**, 797 (2002).
- [10] V. D. Mello, L. I. Zawislak, J. B. M. da Cunha, E. J. Kinast, J. B. Soares, and C. A. dos Santos, J. Magn. Magn. Mater. **196-197**, 846 (1999).
- [11] V. Antonietti, E. J. Kinast, L. I. Zawislak, J. B. M. da Cunha, and C. A. dos Santos, J. Phys. Chem. Solids **62**, 1239 (2001).
- [12] S. M. Eicher, J. E. Greedan, and K. J. Lushington, J. Solid State Chem. **62**, 220 (1986).
- [13] J. N. Reimers, J. E. Greedan, C. V. Stager, and R. Kremer, J. Solid State Chem. **83**, 20 (1989).
- [14] J. Rodriguez-Carvajal, Physica (Amsterdam) **192B**, 55 (1993).
- [15] L. I. Zawislak, G. L. F. Fraga, J. B. Marimon da Cunha, D. Schmitt, A. S. Carriço, and C. A. dos Santos, J. Phys. Condens. Matter **9**, 2295 (1997).
- [16] Y. Muraoka, T. Idogaki, and N. Uryu, J. Phys. Soc. Jpn. **57**, 1758 (1988).
- [17] R. K. Kremer, J. E. Greedan, E. Gmelin, W. Dai, M. A. White, S. M. Eicher, and K. J. Lushington, J. Phys. (France) **49**, 1495 (1988).
- [18] M. Saes, N. P. Raju, and J. E. Greedan, J. Solid State Chem. **140**, 7 (1998).